Journal of Industrial and Engineering Chemistry xxx (xxxx) xxx

Contents lists available at ScienceDirect

Journal of Industrial and Engineering Chemistry

journal homepage: www.elsevier.com/locate/jiec

Short Communication

Industrial-scale chemical synthesis of gold nanorods: process optimization and 30 L scale-up toward GMP manufacturing

Filippo Capancioni [a], Emanuela Bua [a], Erica Locatelli [a], Richard Jasinski [b], David Perrey [c], Tia Cervarich [c], Mauro Comes Franchini [a,*]

[a] Department of Industrial Chemistry "Toso Montanari", Via Gobetti 85, Bologna 40129, Italy
[b] Richman Chemical Inc, 768 N Bethlehem Pike, Suite 204, Lower Gwynedd, PA 19002, United States
[c] Raybow USA, Inc, 158 McLean Road Brevard, NC 28712, United States

ARTICLE INFO

Keywords:
Gold nanorods
Scale-up
Nanostructure scale-up

ABSTRACT

Gold nanorods (GNRs) offer unique photonic properties but remain challenging to reproduce and scale beyond bench volumes. We identify the critical process parameters (CPPs) governing the seed-mediated synthesis of CTAB-stabilized GNRs and translate the process from 30 mL to 30 L. Silver nitrate loading, seed formation (temperature and $NaBH_4$-addition mixing), and growth-phase hydrodynamics emerge as key drivers of the longitudinal LSPR (LLSPR). Tight control of seed temperature and vigorous mixing during reductant addition yield batch-to-batch LLSPR variations within ± 20 nm; introducing gentle agitation during growth suppresses uncontrolled thermal convection, further improving robustness. The optimized protocol produces optically consistent GNRs at 3 L and 30 L with plasmonic features comparable to lab scale. Beyond the experimental advance, this work frames an industrially relevant route to large-scale chemical production of GNRs, establishing process understanding, reproducibility, and quality criteria that underpin future GMP manufacturing design and ongoing regulatory interactions.

Introduction

Over the last decade, gold nanorods have gained widespread recognition as one of the most promising nanostructures for various applications. Their attractiveness mainly lies in their unique optical properties, showing a particular NIR-VIS absorption due to the longitudinal localized surface plasmonic resonance (LLSPR) that depends on the aspect ratio (AR, length to width ratio) of the nanoparticles [1]. This parameter can be easily modified by varying reagent concentrations and reaction parameters, thereby obtaining different ARs for the desired purposes. Thanks to their excellent plasmonic properties, numerous GNR applications have been studied, ranging from optics to other disciplines such as biotechnology, chemistry, and medicine [2]. Particularly, large interest has emerged for GNRs use in cancer diagnostics and treatment: a LLSPR centred in the so-called "biological window", which is the optical wavelengths range in the near-infrared (NIR, 700–1500 nm) characterized by high tissue transparency, allows properly engineered GNRs to be applied for precise visualization of tumour cells and treatment [3–5]. Photoacoustic imaging (PAI) recently arose as one of the most promising options for cancer diagnostics using GNRs: this technique, based on the conversion of optical energy into a wide-band ultrasound wave originated from GNRs acting as photoabsorbers, generates a rapid thermoelastic expansion of tissues that can be detected with a transducer for precise cancer imaging [6]. At the same time, GNRs photoactivity haa been largely applied in photothermal (PTT) and photodynamic therapy (PDT), exploiting the high photochemical efficiency (PCE) of GNRs in converting NIR radiations into heat, able to cause cancer cells necrosis with low systemic toxicity and invasivity [7–9].

Starting from pioneeristic studies by El-Sayed [10], Gole [11], and Wang [12], the seed-mediated growth solution method was widely studied and optimized, trying to obtain robust protocols for reproducible nanoparticles synthesis. This method relies on the anisotropic growth of rod-shaped nanoparticles obtained by the selective interaction between cationic surfactant CTAB and $AgNO_3$ onto specific facets of the gold nanoparticles, which causes aggregation onto the uncoated ones: in particular, isotropic gold seeds added to the growth solution undergo symmetry breaking through gold crystal twinning favoured on exposed

* Corresponding author.
E-mail address: mauro.comesfranchini@unibo.it (M. Comes Franchini).

https://doi.org/10.1016/j.jiec.2026.01.034
Received 24 October 2025; Received in revised form 16 December 2025; Accepted 14 January 2026
Available online 17 January 2026
1226-086X/© 2026 The Author(s). Published by Elsevier B.V. on behalf of The Korean Society of Industrial and Engineering Chemistry. This is an open access article under the CC BY license (http://creativecommons.org/licenses/by/4.0/).

[111] facet, while higher surface energy of [100] and [110] facets causes CTAB binding and surfactant bilayer formation on them, preventing the growth on these [13]. Moreover, the use of a mild-reducing agent such as the ascorbic acid instead of a stronger agent like $NaBH_4$ in growth solution arrests the tendency of nucleation in growth solution and facilitates the growth of added seeds into anisotropic structures [14].

Many different studies focused on the main parameters regulating the anisotropic growth, like surfactant characteristics [15], pH [16], $AgNO_3$[17], seed solution [14], and ascorbic acid amount [18]. Design of experiment (DOE) has also been applied, underlining the complex interactions between different reaction parameters [19,20], but the lack of reproducibility in GNRs dimensions and optical absorption is still considered the main issue of the synthesis, limiting their large-scale production and effective application for biomedical purposes. Some studies in literature reported the attempt to scale up GNRs synthesis to larger volumes than lab-scale, but results are still far from pilot-like plants suitable for future industrial productions [21–24]. Additionally, even if many nanomedicine technologies are nowadays commonly produced in large-scale amounts [25], gold nanoparticle synthesis in the biomedical field is still mainly made by top-down approaches like microwaves, UV irradiation, and other physical methods [26]. The principal drawback of these processes, besides the higher energetic costs, is the lack of dimensional fine tuning allowed by chemical methods, well assessed at lab scale but still difficult to apply at larger scales [27].

In this context, the development of a reproducible and scalable chemical route for the synthesis of gold nanorods represents a key step toward their industrial translation. Although many reports have optimized laboratory-scale syntheses, few have addressed the engineering challenges that emerge when volumes and mass transfer dynamics are extended beyond bench scale. Large-scale nanomaterial production requires the definition of critical process parameters (CPPs) and critical quality attributes (CQAs) ensuring dimensional control, optical consistency, and batch-to-batch reproducibility. The ability to scale up complex colloidal systems such as CTAB-stabilized gold nanorods without compromising their longitudinal plasmonic response is particularly demanding due to nonlinear effects in nucleation, seed growth, and mixing regimes [28].

Therefore, this study not only aims to optimize the physicochemical synthesis parameters, but also to provide a robust industrial-grade process, understanding the bridges that laboratory chemistry and future Good Manufacturing Practice (GMP) design. By identifying and controlling the variables most influencing the longitudinal localized surface plasmon resonance (LLSPR), we establish the technical foundation required for regulatory translation and for future GMP manufacturing strategies.

Experimental section

Materials

Cetyltrimethylammonium bromide, sodium oleate, tetrachloroauric acid were purchased from BLD Pharmatech GmbH (Reinbeck, Germany). Silver nitrate, ascorbic acid, hydrochloric acid 37 % and sodium borohydride were purchased from Sigma-Aldrich (St. Louis, MO, USA).

Ctab-coated gold nanorods (GNRs@CTAB) synthesis and characterization

Cetyltrimethylammonium bromide (CTAB)-coated GNRs (GNRs@CTAB) with a maximum absorption at 770–850 nm, were prepared according to a previously published procedure with minor modifications [4]. In a 500 mL one-neck round bottom flask, growth solution was first synthesized. CTAB (5.19 g, 47.5 mM) and sodium oleate (0.71 g, 7.8 mM) were dissolved in USP-grade water (300 mL) at 50 °C. Once all solids were dissolved, the solution was cooled down to 30 °C and broken into 30 mL aliquots that were maintained at 30 °C throughout the synthesis (growth solutions). With gentle stirring (350 rpm), AgNO3 (0.1 M) was added to each aliquot, then the stirring was stopped, and the solutions were allowed to age for 15 min. Under vigorous stirring (700 rpm), 0.144 mL of a 0.1 M HAuCl4 solution was added to each aliquot. After 90 min of stirring, 0.059 mL of HCl (37 wt%) was added, then 0.059 mL of ascorbic acid (0.08 M) was added after 15 min, followed by the seed solution under vigorous stirring for 30 min. Parallelly, the seed solution was synthesized by dissolving CTAB (364 mg, 0.1 M) in USP-grade water (10 mL) at about 50 °C. Then, with vigorous stirring and maintaining the solution at 30 °C, HAuCl4 (0.1 M, 25 μL) was added. Once a homogeneous yellow solution was obtained, ice-cold NaBH4 (0.01 M, 600 μL) was added, the solution was stirred for 30 s, then allowed to age without stirring for 30 min before the addition into the growth solution. Once the growth solutions stirring ceased, solutions were allowed to age at 30 °C overnight.

The GNRs@CTAB synthesis was then scaled up by 10x (300 mL), 100x (3 L), and 1000x (30 L) factors, using optimized equivalents of reagents as those used for the 30 mL scale.

Purification of GNRs@CTAB obtained from 30 mL, 300 mL and 3 L scale was performed by using a Sartorius Centrisart G-16 centrifuge in 50-mL Falcon tubes (6,000 rpm for 100 min, 25 °C), by removing 40 mL of the supernatant and re-dispersion of centrifuged pellet in 40 mL of ultrapure water, and the process was repeated 3 times. GNRs@CTAB obtained from 30 L reactions were purified using a Sorvall RC-5B Refrigerated Superspeed Centrifuge. The solution was centrifuged at 10,800 x g (8,000 rpm) at 25 °C in PPCO centrifuge bottles (6 x 400 mL) for 60 min, then the supernatant was removed, leaving about 30 mL of concentrated GNR solution per bottle. The concentrated solutions were combined and set aside. This process was repeated until the full solution had been concentrated (centrifuged 13 times over 4 days; the reaction solution was stored at 30 °C before centrifugation, and the concentrated GNR solution was stored at ambient temperature). The concentrated GNR solution (~2.4 L) was centrifuged at 6,090 x g (6,000 rpm) for 90 min, then all but ~ 50 mL of the supernatant was removed. The concentrated GNR solution was combined and diluted to 3 L with USP-grade water.

CTAB quantification in concentrated GNRs was obtained via HPLC measurements using an Agilent 1260 HPLC with Thermo Scientific Corona Veo Charged Aerosol Detector (Agilent Technologies, Santa Clara, USA). CTAB concentration values measured are reported in Table S1.

The UV–vis were obtained by diluting 0.5 mL of the reaction solution with 1.5 mL of USP-grade water, using a Cary 3500 UV–VIS–NIR modular spectrometer (Agilent Technologies, Santa Clara, USA) using a 1 cm path-length plastic cuvette (range 400–1000 nm).

Gold concentration was determined by flame atomic absorption spectroscopy (FAAS) using a SpectraAA 100 Varian spectrometer (Agilent Technologies, Santa Clara, USA). Gold nanorods (100 μL) were dissolved in H_2O/HNO_3 50/50 w/w solution (10 mL) prior to analysis. For the calibration of the FAAS analysis, Au standard solutions at 1, 2, 5 and 10 mg/L were prepared by diluting the appropriate amounts of 1000 mg/ml TraceCERT® solutions in H_2O/HNO_3 50/50 w/w solution.

Results and Discussion

Effect of AgNO3

The first parameter considered for understanding the tuning of GNRs@CTAB LLSPR wavelength was the amount of silver nitrate. Literature offers many examples of the silver nitrate role in GNRs growth as a templating agent, able to cause anisotropic aggregation of gold nanoparticles and forming rod-like shapes. In particular, it is largely reported that increasing amounts of $AgNO_3$ result in red-shifting of GNRs LLSPR [29]. This aspect was also confirmed by our tests, in which different equivalents of $AgNO_3$ (referred to $HAuCl_4$) were added to growth solutions, obtaining a trend of LLSPR red-shift by increasing the

silver amount (Fig. 1a). Even if $AgNO_3$ equivalents showed a clear effect on GNRs LLSPR, poor batch-by-batch reproducibility was observed. Indeed, reactions set up on different days using the same amount of $AgNO_3$ gave significantly different results (Fig. 1b). Therefore, it was concluded that while the amount of silver does affect the reaction outcome, it was not the main variable in controlling its reproducibility. Additionally, at higher $AgNO_3$ equivalents than 0.48 relative to $HAuCl_4$, formation of a white precipitate was observed that persisted throughout the reaction, probably deriving from Ag^+ interacting with Br^- coming from the surfactant and precipitating in AgBr salt, as also reported in literatures [10,17]. This meant that we could not push the silver concentration over a certain amount to produce GNRs with the desired wavelength without the formation of the precipitate as well.

Effect of seed solution

According to literature, seed solution characteristics have a huge effect on the final absorption wavelength of GNRs. Increasing amounts of seeds added to the growth solution are generally associated with increasing red shifts, while lowering seed solution synthesis temperature results in a final blue shift of GNRs LLSPR [28]. This general trend was confirmed by the results reported (Fig. 2, S1), in which increased amounts of seeds caused LLSPR red-shift, while the same amount of seed solution obtained with lower temperatures caused LLSPR blue-shifts of 30 nm or even more.

While the observed trend (increasing seed causes a red shift in LSPR wavelength) was reproducible from day to day, we found that the wavelength obtained using a specific volume of seed varied significantly between different batches of seed (Fig. 3a). A single batch of seed gave reproducible results, but even two batches of seed synthesized in parallel (same water bath, same stir rate) could produce GNRs that differed by more than 20 nm. We hypothesized that this may be due to differences in mixing during the $NaBH_4$ addition. The literature emphasizes that the $NaBH_4$ addition should be "instantaneous" so that the gold is reduced evenly across the solution, but no strategies have been proposed to perform this in a reproducible way. To facilitate this, the stir rate of the

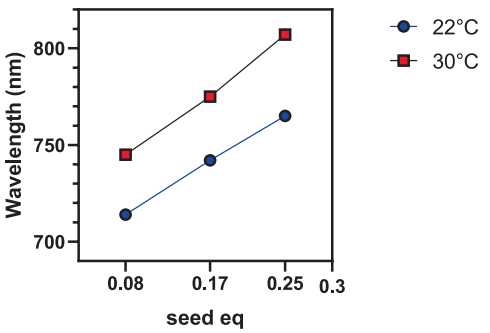

Fig. 2. Effect of increased amount of seed solution (seed eq. = seed mL/HAuCl4 0.1 M mL) at different temperatures.

seed solution during the $NaBH_4$ addition was increased from 700 rpm (vigorous stirring with a controlled vortex) to 1500 rpm (vigorous stirring with an uncontrolled, chaotic vortex). Increased turbolent regime was evaluated by Reynolds number calculations (Table S2) and allowed to obtain multiple batches of seed prepared in parallel giving more consistent results (Fig. 3b).

The optimal equivalents of seed were determined to be 36 μL (0.25 volumetric equivalents relative to $HAuCl_4$ solution) as it gave GNRs with a wavelength of 790–815 nm. To further elucidate the effect of seed temperature, different syntheses varying the seed amount and the temperature were performed. We observed that the temperature of the seed has a bigger effect on the stirred reactions reproducibility than the seed amount does. Forming the seed at temperatures lower than 30 °C causes a blue-shift of the GNRs produced, while forming the seed at either 19 °C or 25 °C led to a blue shift of > 50 nm compared to seed formed at 30 °C (Fig. S2). A possible explanation of this aspect could lie in the temperature dependency of $NaBH_4$ reduction rate. It is largely reported that higher temperatures in gold reduction lead to higher nanoparticle yield [30], resulting in a higher number of seeds and consequently in a general increase of AR of GNRs [11]. Thus, precise control of seed solution temperature at 30 °C allows a more complete

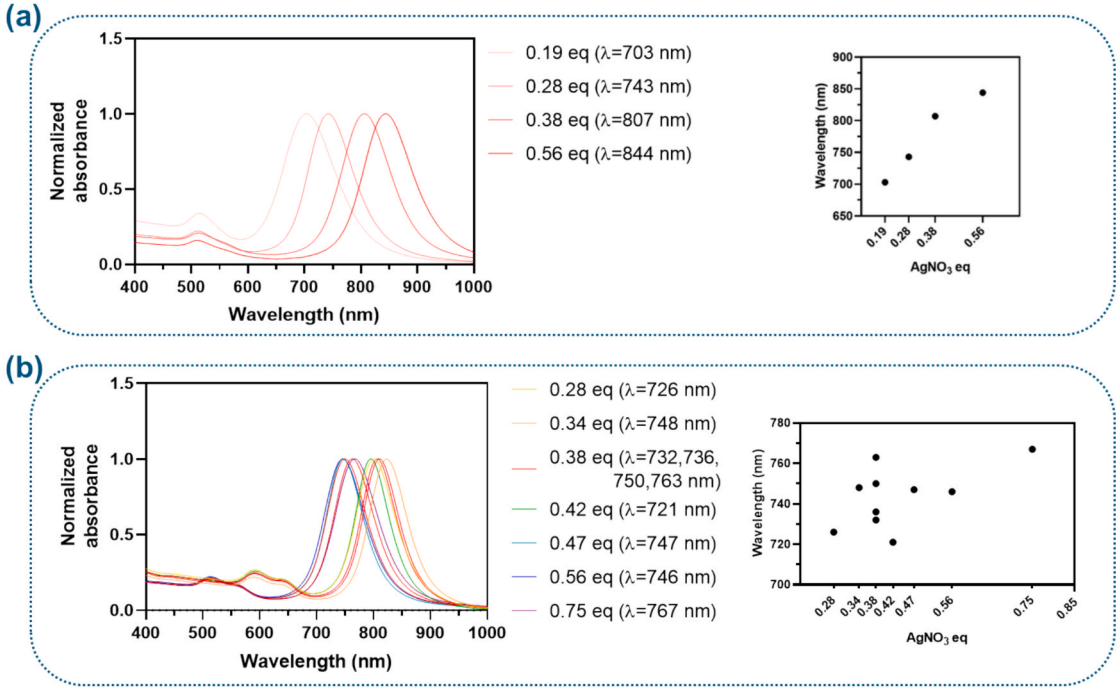

Fig. 1. (a) Effect of $AgNO_3$ equivalents on LLSPR wavelength (*referred to $HAuCl_4$). (b) Effect of $AgNO_3$ equivalents on LLSPR wavelength in different days. Poor reproducibility connected with the variation of only the $AgNO_3$ equivalents is shown by the non-linear correlation between wavelength and $AgNO_3$, represented by the graph on the right.

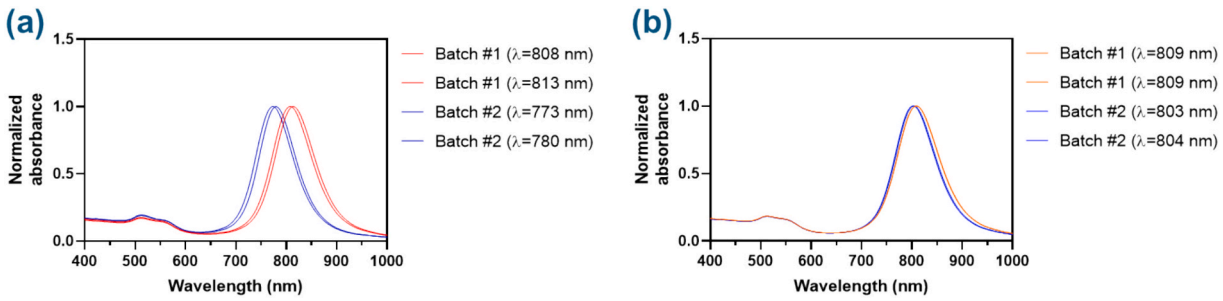

Fig. 3. (a) Effect of different seed batches on LLSPR reproducibility, using same amount of seed equivalents (0.25 equivalents) and same temperature (30 °C). (b) Effect of increased stirring rate during $NaBH_4$ addition on LLSPR reproducibility using different batches of seed solution.

reduction of the chloric acid used in the seed solution and a higher reproducibility of the final GNRs LLSPR. In addition, CTAB precipitation occurs at temperatures below 25 °C, causing crystallite formation that could interfere rod growth [31]. Therefore, a higher seed solution temperature appears to prevent uncontrolled crystallites from inhibit gold nanorods formation.

Scale up

Once reproducible conditions that yielded GNRs with a LSPR band around 800–810 nm had been found, the reaction was scaled up by a factor of ten to a 300 mL scale (135 μL 0.4 M $AgNO_3$, 1.44 mL 0.1 M $HAuCl_4$, 587 μL 0.08 M ascorbic acid, 592 μL 37 wt% HCl, 360 μL seed). Initial results at this scale indicated that the conditions used for the 30 mL probe reactions would successfully translate to 300 mL, but repeated reactions on this scale failed to replicate these results with a broad distribution of LLSPR (Fig. S3). After examining several variables, we concluded that this irreproducibility was likely caused by random variances in thermal mixing during the growth stage of the reaction. Since the reaction was not stirred during the growth stage, variations in temperature throughout the solution led to uncontrolled mixing by convection. The rate of mixing will be affected by variables such as the ambient temperature and the depth of the water bath, and it is thus difficult to fully control. To avoid this problem, we examined how a slow stirring during the growth phase would affect the reaction. Repeating the conditions used for the non-stirred reactions but stirring the growth solution at a rate of ~ 10 rpm yielded gold nanorods with an LLSPR band more difficult to perturb than non-stirred reactions, generally falling between 830–845 nm regardless of how much seed was added (Fig. 4).

Once all the considered parameters have been studied and optimized, scale-up at 3 and 30 L scale have been conducted. Results of the obtained reactions, with underlined spectral window desired, are reported in Fig. 5, while TEM analyses of GNRs sizes confirming the consistency of the scale-up are reported in Fig. S5. An average AR of 3.96 ± 0.43 and average LLSPR wavelength of 836 ± 8 nm (Table S3) is obtained through the scale-ups, with a LLSPR difference smaller than 20 nm between the three batches, similarly with the ones obtained from smaller scale reactions. Reproducible gold yield was assessed, as reported by FAAS analyses giving an average yield of 43 % (Table S4), consistent with values already collected in past works by our research group [4].

Conclusions

In this work, we examined the effect of the main critical process parameters of GNRs synthesis, focusing on LLSPR reproducibility for large scale productions. $AgNO_3$ amount, seed solutions properties and physical miscelation were mainly take in account for their direct effect on tuning GNRs aspect ratio and LLSPR wavelength, as shown in the summarized results collected in Table S5. While $AgNO_3$ was confirmed to have a clear effect on increasing GNRs AR, it was found that it poorly influenced LLSPR reproducibility. A major impact on this parameter is given by the seed solution: in accordance with literature, we confirmed the general red-shift obtained by increasing the seed amount, but we additionally found out that increased seed synthesis temperature and stirring rate during $NaBH_4$ addition led to higher reproducibility because of a more complete gold reduction into seeds. Finally, slow stirring during GNRs growth step was found to limit uncontrolled thermal mixing and to further increase the robustness of the synthesis when moving to larger scales. In addition, we applied these optimized parameters for 3 L and 30 L synthesis, trying to simulate a pilot scale process for the obtainment of these materials: to the best of our knowledge, few 30 L scaled seed-mediated gold nanorods synthesis have been reported, and this work seems opening the possibility to obtain GNRs in big amounts with reproducible features for future biomedical applications.

Beyond the scientific outcome, the industrial relevance of this work

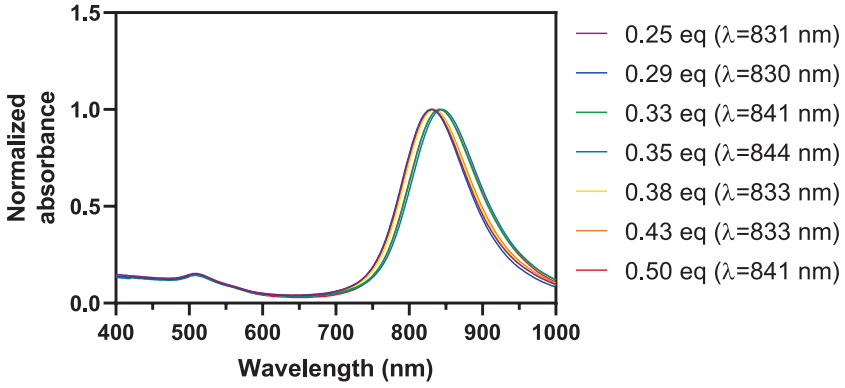

Fig. 4. Effect of slow stirring rate (10 rpm) during growth step on LLSPR reproducibility. Proper mixing during growth step results crucial in increased LLSPR reproducibility, as synthesis made with different seed solution equivalents yielded GNRs with LLSPR ranging from 831 to 844 nm.

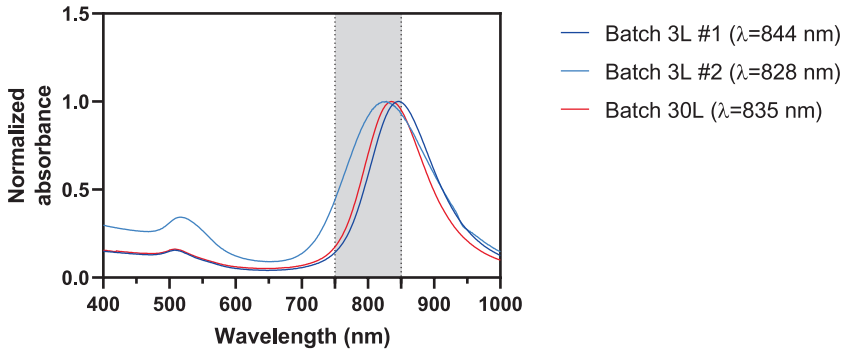

Fig. 5. LLSPR of scaled-up GNRs synthesis. Average LLSPR of 836 ± 8 is obtained from the three different scaled-up reactions (Table S3).

lies in demonstrating that the chemical seed-mediated route can be transferred to a 30 L scale while maintaining process robustness and product reproducibility. This achievement provides the quantitative understanding of process variability, yield, and optical performance required to design GMP-compliant production schemes.

The identification of the critical process parameters — seed formation dynamics, thermal homogeneity, and controlled mixing — constitutes a necessary milestone for the forthcoming regulatory dialogue with competent authorities. In fact, the process optimization described here has been depicted in the preparation of the scientific advice request to the European Medicines Agency (EMA), thus positioning this scaled-up synthesis as the enabling step for future clinical translation of gold-nanorod-based nanomedicines.

CRediT authorship contribution statement

Filippo Capancioni: Writing – review & editing, Writing – original draft, Methodology, Investigation, Formal analysis, Data curation, Conceptualization. **Emanuela Bua:** Writing – review & editing, Writing – original draft, Methodology, Investigation, Formal analysis, Data curation, Conceptualization. **Erica Locatelli:** Writing – review & editing, Validation, Supervision, Methodology, Conceptualization. **Richard Jasinski:** Writing – review & editing, Validation, Supervision, Resources, Conceptualization. **David Perrey:** Writing – review & editing, Validation, Methodology, Data curation. **Tia Cervarich:** Methodology, Investigation, Formal analysis, Data curation. **Mauro Comes Franchini:** Writing – review & editing, Validation, Supervision, Resources, Funding acquisition, Conceptualization.

Declaration of competing interest

The authors declare that they have no known competing financial interests or personal relationships that could have appeared to influence the work reported in this paper.

Acknowledgements

This work was made possible through funding from the European Union. Views and opinions expressed are those of the author(s) and do not necessarily reflect those of the EU or the EIC. PHIRE project is funded under Grant Agreement ID No. 101113193.

Appendix A. Supplementary data

Supplementary data to this article can be found online at https://doi.org/10.1016/j.jiec.2026.01.034.

References

[1] J. Cao, T. Sun, K.T. Grattan, Sens. Actuators B 195 (2014) 332–351.
[2] M. Maturi,, E. Locatelli,, I. Monaco,, M. Comes Franchini, Biomater. Sci. 7(5) (2019) 1746–75. 10.1039/C8BM01444B.
[3] J. Weber, P.C. Beard, S.E. Bohndiek, Nat. Methods 13 (8) (2016) 639–650.
[4] E. Alchera, M. Monieri, M. Maturi, I. Locatelli, E. Locatelli, S. Tortorella, A. Sacchi, A. Corti, M. Nebuloni, R. Lucianò, F. Pederzoli, F. Montorsi, A. Salonia, S. Meyer, J. Jose, P. Giustetto, M.C. Franchini, F. Curnis, M. Alfano, Photoacoustics 28 (2022) 100400, https://doi.org/10.1016/j.pacs.2022.100400.
[5] C. Venegoni, S. Tortorella, A. Caliendo, I. Locatelli, A.D. Coste, E. Locatelli, F. Capancioni, E. Bua, S. Camorani, A. Salonia, F. Montorsi, J. Jose, M. Moschini, L. Cerchia, M.C. Franchini, M. Alfano, Adv. Healthc. Mater. 14 (10) (2025) 2403314, https://doi.org/10.1002/adhm.202403314.
[6] W. Li, X. Chen, Nanomedicine 10 (2) (2015) 299–320.
[7] S. Liao, W. Yue, S. Cai, Q. Tang, W. Lu, L. Huang, T. Qi, J. Liao, Front. Pharmacol. 12 (2021) 664123.
[8] L. Tong, Q. Wei, A. Wei, J. Cheng, Photochem. Photobiol. 85 (1) (2009) 21–32, https://doi.org/10.1111/j.1751-1097.2008.00507.x.
[9] A.-G. Niculescu, A.M. Grumezescu, Appl. Sci. 11 (8) (2021) 3626.
[10] B. Nikoobakht, M.A. El-Sayed, Chem. Mater. 15 (10) (2003) 1957–1962.
[11] A. Gole, C.J. Murphy, Chem. Mater. 16 (19) (2004) 3633–3640, https://doi.org/10.1021/cm0492336.
[12] H. Chen, L. Shao, Q. Li, J. Wang, Chem. Soc. Rev. 42 (7) (2013) 2679–2724.
[13] A. Chhatre, R. Thaokar, A. Mehra, Cryst. Growth Des. 18 (6) (2018) 3269–3282.
[14] N.R. Jana, L. Gearheart, C.J. Murphy, Adv. Mater. 13 (18) (2001) 1389–1393.
[15] X. Ye, C. Zheng, J. Chen, Y. Gao, C.B. Murray, Nano Lett. 13 (2) (2013) 765–771.
[16] J. Cheng, L. Ge, B. Xiong, Y. He, J. Chin. Chem. Soc. 58 (6) (2011) 822–827, https://doi.org/10.1002/jccs.201190128.
[17] W. Tong, M.J. Walsh, P. Mulvaney, J. Etheridge, A.M. Funston, J. Phys. Chem. C 121 (6) (2017) 3549–3559, https://doi.org/10.1021/acs.jpcc.6b10343.
[18] Z. Khan, T. Singh, J.I. Hussain, A.A. Hashmi, Colloids Surf. B Biointerfaces 104 (2013) 11–17.
[19] M.R. Hormozi-Nezhad, H. Robatjazi, M. Jalali-Heravi, Anal. Chim. Acta 779 (2013) 14–21.
[20] N.D. Burrows, S. Harvey, F.A. Idesis, C.J. Murphy, Langmuir 33 (8) (2017) 1891–1907.
[21] N.R. Jana, Small 1 (8–9) (2005) 875–882.
[22] N.R. Jana, X. Peng, J. Am. Chem. Soc. 125 (47) (2003) 14280–14281.
[23] K.A. Kozek, K.M. Kozek, W.-C. Wu, S.R. Mishra, J.B. Tracy, Chem. Mater. 25 (22) (2013) 4537–4544.
[24] C. Yan, Y. Wang, Q. Tian, H. Wu, S. Yang, Mater. Sci. Eng. C 87 (2018) 120–127.
[25] D.N. Heo, K.H. Min, G.H. Choi, I.K. Kwon, K. Park, S.C. Lee, Cancer Theranostics (2014) 457–470.
[26] R. Paliwal, R.J. Babu, S. Palakurthi, AAPS PharmSciTech 15 (6) (2014) 1527–1534.
[27] N. Abid, A.M. Khan, S. Shujait, K. Chaudhary, M. Ikram, M. Imran, J. Haider, M. Khan, Q. Khan, M. Maqbool, Adv. Colloid Interface Sci. 300 (2022) 102597.
[28] S. Yoon, B. Lee, J. Yun, J.G. Han, J.-S. Lee, J.H. Lee, Nanoscale 9 (21) (2017) 7114–7123, https://doi.org/10.1039/C7NR01462G.
[29] J. Pérez-Juste, I. Pastoriza-Santos, L.M. Liz-Marzán, P. Mulvaney, Coord. Chem. Rev. 249 (17–18) (2005) 1870–1901, https://doi.org/10.1016/j.ccr.2005.01.030.
[30] G. Mountrichas, S. Pispas, E.I. Kamitsos, J. Phys. Chem. C 118 (39) (2014) 22754–22759.
[31] X. Liu, J. Yao, J. Luo, X. Duan, Y. Yao, T. Liu, Langmuir 33 (30) (2017) 7479–7485.